

Contents lists available at [SciVerse ScienceDirect](http://www.sciencedirect.com)

Spectrochimica Acta Part A: Molecular and Biomolecular Spectroscopy

journal homepage: www.elsevier.com/locate/saa

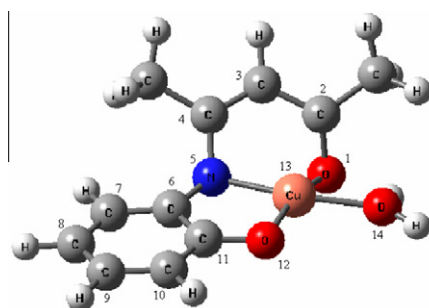
Synthesis, spectroscopy, electrochemistry and thermogravimetry of copper(II) tridentate Schiff base complexes, theoretical study of the structures of compounds and kinetic study of the tautomerism reactions by ab initio calculations

Ali Hossein Kianfar^{a,*}, Shapour Ramazani^b, Roghaye Hashemi Fath^c, Mahmoud Roushani^d^a Department of Chemistry, Isfahan University of Technology, Isfahan 84156-83111, Iran^b Department of Chemistry, Yasouj University, Yasouj, Iran^c Young Researchers Club, Gachsaran Branch, Islamic Azad University, Gachsaran, Iran^d Department of Chemistry, Ilam University, Ilam, Iran

HIGHLIGHTS

- ▶ The new complexes were synthesized by a simple method.
- ▶ Article contains some scopes like ab initio calculations of ligands and complexes.
- ▶ The ligands exist as keto-amine/enol-imine tautomeric forms.
- ▶ Cu(II) ion is in square-planar NO₃ coordination geometry.
- ▶ Paper contains Inorganic, organic, analytical and physical chemistry.

GRAPHICAL ABSTRACT



ARTICLE INFO

Article history:

Received 23 October 2012

Received in revised form 2 December 2012

Accepted 6 December 2012

Available online 28 December 2012

Keywords:

Schiff base ligands

Copper Schiff base complexes

Electrochemistry: thermogravimetry

Ab initio calculations

ABSTRACT

Attempts to spectroscopic and structural study of copper complexes, some Cu(II) Schiff base complexes were synthesized and characterized by means of electronic, IR, ¹HNMR spectra and elemental analysis. The thermal analyses of the complexes were investigated and the first order kinetic parameters were derived for them. The cyclic voltammetric studies in acetonitrile were proposed a monomeric structure for complexes. The structures of compounds were determined by ab initio calculations. In the solid state, the ligands exist as keto-amine/enol-imine tautomeric forms with an intramolecular hydrogen bond (N–H···O) between amine and carbonyl group. The kinetic studies of the tautomerism and equilibrium constant of the reactions were calculated using transition state theory. The optimized molecular geometry and atomic charges were calculated using MP2 method with 6-31G(d) basis set for H, C, N and O atoms and LANL2DZ for the Cu atom.

The results suggested that, in the complexes, Cu(II) ion is in pseudo square-planar NO₃ coordination geometry. Also the bond lengths and angles were studied and compared.

© 2012 Elsevier B.V. All rights reserved.

Introduction

Schiff bases have been widely used as ligands because of the high stability of coordination compounds with different oxidation

* Corresponding author. Tel.: +98 311 3913251; fax: +98 311 3912350.

E-mail addresses: akianfar@cc.iut.ac.ir, asarvestani@yahoo.com (A.H. Kianfar), ramazani@mail.yu.ac.ir (S. Ramazani).

states. The π -system in a Schiff base often imposes a geometrical constriction and affects the electronic structure as well. Transition metal Schiff base complexes have been studied as catalysts in organic redox and electrochemical reduction reactions [1–5]. Transition metal complexes are important in many areas of science, including catalysis, medicine, modifier of nanostructure compounds, design of high value materials, analytical chemistry. In addition, they are used as model compounds of the structure

and function of metalloproteins [6–10]. The keto-amine/enol-imine tautomerism is reported for Schiff bases derived from β -diketones [11,12]. The theoretical study of Schiff bases with tautomerism forms were investigated previously [13,14].

The present study describes the synthesis of Schiff base ligands derived from the reactions of acetylacetone with 2-aminophenol and 2-amino-4-chlorophenol and the reaction of benzoylacetone with 2-aminophenol. The copper(II) complexes of synthesized ligands were prepared in methanol (Figs. 1 and 2) and identified by IR, NMR, UV–Vis spectroscopy and elemental analysis. The thermal analyses of the studied complexes were investigated. From thermal decomposition data, the kinetic's parameters were calculated using Coats and Redfern [15] method. The structures of compounds were determined by ab initio calculations. The keto-amine/enol-imine conversion was investigated by ab initio quantum chemical calculations in order to reveal the stability of the different tautomers and the possible formation of order conformers. The conjugation of the different tautomers was examined in order to understand the differences in their relative stability. The kinetic studies of the tautomerism and equilibrium constant of the reactions were calculated using transition state theory. The optimized molecular geometry and atomic charges were calculated using MP2 method with 6-31G(d) basis set for H, C, N and O atoms and LANL2DZ for the Cu atom.

Experimental

Chemicals and apparatus

All of the chemicals and solvents used for the synthesis were of commercially available reagent grade and they were used without purification. Infrared spectra were recorded as KBr discs on a FT-IR JASCO-680 spectrophotometer in the 4000–400 cm^{-1} . The elemental analysis was determined on a CHN-O-Heraeus elemental analyzer. UV–Vis spectra were recorded on a JASCO V-570 spectrophotometer in the 190–900 nm. The ^1H NMR spectra were recorded in DMSO- d_6 on DPX-400 MHz FT-NMR. Thermogravimetry (TG) and differential thermoanalysis (DTA) were carried out on a PL-1500. The measurements were performed in air atmosphere. The heating rate was kept at 10 $^\circ\text{C min}^{-1}$.

Cyclic voltammograms were performed using an autolab modular electrochemical system (ECO Chemie, Utrecht, The Netherlands) equipped with a PSTA 20 module and driven by GPES (ECO Chemie) in conjunction with a three-electrode system and a personal computer for data storage and processing. An Ag/AgCl (saturated KCl)/3 M KCl reference electrode, a Pt wire as counter electrode and a glassy carbon electrode as working electrode

(metrom glassy carbon, 0.0314 cm^2) were employed for the electrochemical studies. Voltammetric measurements were performed at room temperature in acetonitrile solution with 0.1 M tetrabutylammonium perchlorate as the supporting electrolyte.

Synthesis of Schiff base ligands

Synthesis of 2-(3-hydroxy-1-methyl-but-2-enylideneamino)-phenol (H_2L^1)

The Schiff base ligand, H_2L^1 , was prepared by adding a methanolic solution of 2-aminophenol (0.546 g, 5 mmol) to acetylacetone (0.514 ml, 5 mmol) in methanol and refluxed for 4 h. The reaction mixture was filtered, reduced to one-third of its original volume, and left to crystallize at room temperature. The light yellow crystals were isolated from the solution and dried in vacuum [10]. Yield: 82%, m.p \approx 183 $^\circ\text{C}$. IR (KBr pellets, cm^{-1}): 3300 (ν_{NH}), 3000 (ν_{OH}), 1600 ($\nu_{\text{C=N/C=O}}$). ^1H NMR (DMSO, δ_{H}): 12.14 (s, 1H, NH/OH), 9.91 (s, 1H, phenolic OH), 6.77–7.16 (m, 4H, Aromatic protons), 5.18 (s, 1H, C(3)–H), 1.99 and 1.94 (s, 6H, CH_3), ppm., λ_{max} (nm) (ϵ , $\text{L mol}^{-1} \text{cm}^{-1}$) (Ethanol): 206 (10000), 233 (3900), 320 (11500).

Synthesis of 2-(3-hydroxy-1-methyl-but-2-enylideneamino)-4-chlorophenol (H_2L^2)

The Schiff base ligand, H_2L^2 , was prepared by adding a methanolic solution of 2-amino-4-chlorophenol (0.718 g, 5 mmol) to acetylacetone (0.514 ml, 5 mmol) in methanol and refluxed for 6 h. The light green crystals were isolated from the solution at room temperature and dried in vacuum. Yield: 79%, m.p \approx 160 $^\circ\text{C}$. IR (KBr pellets, cm^{-1}): 3100–2400 ($\nu_{\text{NH/OH}}$), 1600 ($\nu_{\text{C=N/C=O}}$). ^1H NMR (DMSO, δ_{H}): 12.14 (s, 1H, NH/OH), 10.24 (s, 1H, phenolic OH), 6.87–7.26 (m, 3H, Aromatic protons), 5.22 (s, 1H, C(3)–H), 2.01 and 1.96 (s, 6H, CH_3), ppm., λ_{max} (nm) (ϵ , $\text{L mol}^{-1} \text{cm}^{-1}$) (Ethanol): 207 (7300), 238 (3300), 326 (7300).

Synthesis of 2-(3-hydroxy-1-methyl-3-phenyl-prop-2-enylideneamino)-phenol (H_2L^3)

The Schiff base ligand, H_2L^3 , was prepared by adding a methanolic solution of 2-aminophenol (0.546 g, 5 mmol) to benzoylacetone (0.811 g, 5 mmol) in methanol and refluxed for 2 h. The yellow crystals were isolated from the solution at room temperature and dried in vacuum. Yield: 84%, m.p \approx 166 $^\circ\text{C}$. IR (KBr pellets, cm^{-1}): 3100–2400 ($\nu_{\text{NH/OH}}$), 1600 ($\nu_{\text{C=N/C=O}}$). ^1H NMR (DMSO, δ_{H}): 12.80 (s, 1H, NH/OH), 10.03 (s, 1H, phenolic OH), 6.96–7.91 (m, 9H, Aromatic protons), 6.02 (s, 1H, C(3)–H), 2.13 (s, 3H, CH_3), ppm., λ_{max} (nm) (ϵ , $\text{L mol}^{-1} \text{cm}^{-1}$) (Ethanol): 206 (25300), 244 (13600), 355 (25700).

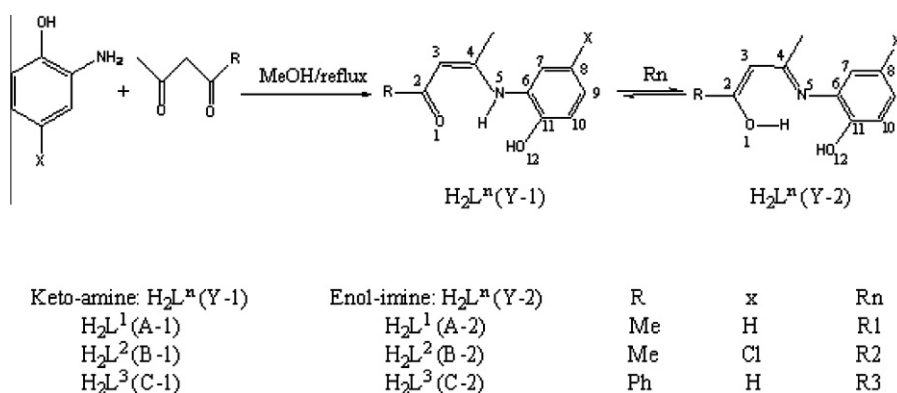


Fig. 1. Structure of Schiff base ligands and their tautomerism equilibrium: keto-amine and enol-imine.

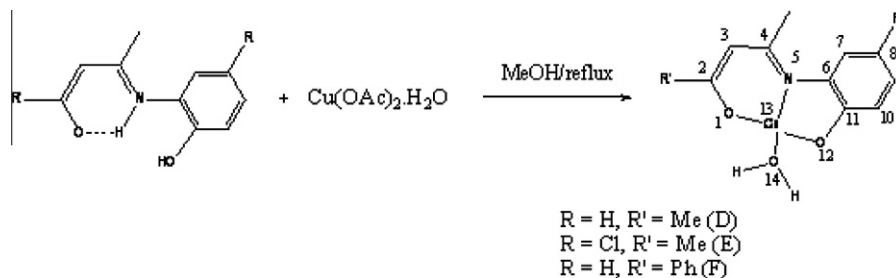


Fig. 2. Proposed molecular structure of metal complexes (D–F).

Metal complexes synthesis

A methanolic solution of the appropriate amount of copper(II)acetate monohydrate was added to a hot methanolic solution of the Schiff base ligand. The resulting mixture was stirred under reflux for 30 min during which the metal complexes were precipitated. The precipitate was filtered off and washed with methanol and dried in vacuum.

[CuL¹(H₂O)] (D) is prepared from Cu(OAc)₂·H₂O (0.4 g, 2 mmol) and H₂L¹ (0.382 g, 2 mmol). Yield: 67%. m.p. ≈ 282 °C. Anal. Calc. for C₁₁H₁₃NO₃Cu: C, 49.82; H, 4.28; N, 6.19. Found: C, 48.79; H, 4.83; N, 5.17%. IR (KBr pellets, cm⁻¹): 1560 (ν_{C=N}), 526 (ν_{Cu-O}), 482 (ν_{Cu-N}). λ_{max} (nm) (ε, L mol⁻¹ cm⁻¹) (Ethanol): 217 (16700), 242 (9900), 275 (9900), 315 (4500), 372 (12900).

[CuL²(H₂O)] (E) was prepared from Cu(OAc)₂·H₂O (0.4 g, 2 mmol) and H₂L² (0.451 g, 2 mmol). Yield: 65%. m.p. ≈ 294 °C. Anal. Calc. for C₁₁H₁₂NO₃ClCu: C, 44.06; H, 3.38; N, 4.36. Found: C, 43.28; H, 4.28; N, 4.58%. IR (KBr pellets, cm⁻¹): 1570 (ν_{C=N}), 540 (ν_{Cu-O}), 480 (ν_{Cu-N}). λ_{max} (nm) (ε, L mol⁻¹ cm⁻¹) (Ethanol): 222 (22500), 245 (16400), 277 (14400), 321 (8400), 377 (18100).

[CuL³(H₂O)] (F) was prepared from Cu(OAc)₂·H₂O (0.4 g, 2 mmol) and H₂L³ (0.506 g, 2 mmol). Yield: 70%. m.p. ≈ 280 °C. Anal. Calc. for C₁₆H₁₅NO₃Cu: C, 58.90; H, 3.98; N, 5.19. Found: C, 57.73; H, 4.53; N, 4.20%. IR (KBr pellets, cm⁻¹): 1580 (ν_{sy(C=N)}), 1560 (ν_{asy(C=N)}), 520 (ν_{Cu-O}), 490 (ν_{Cu-N}). λ_{max} (nm) (ε, L mol⁻¹ cm⁻¹) (Ethanol): 212 (14900), 254 (15200), 278 (12800), 332 (8200), 407 (17100).

Computational calculations

Ab initio calculations were carried out using the Gaussian 03 program [16]. The geometries of all the stationary points were optimized at the MP2 [16] level with the 6-31G(d) basis set for H, C, N and O atoms and LANL2DZ for the Cu atom. Harmonic vibrational frequencies were obtained at B3LYP/6-31G(d) level in order to characterize stationary points as local minima or first-order saddle points. The number of imaginary frequencies (0 or 1) indicate whether a minimum or a transition state was located. The atomic charges were calculated at the MP2 method with 6-31G(d) basis set.

Results and discussion

IR spectra

The mode of binding Schiff base ligands to the metal ions was elucidated by recording the IR spectra of the complexes as compared with the spectra of the free ligands [17]. A keto-amine/enol-imine structure for Schiff-base ligands derived from diketones and diamines was proposed and shows that the hydrogen is bonded to both oxygen and nitrogen simultaneously (NH/OH) [18–21]. The vibrational band of (NH/OH) is observed in the range

of 2400–3300 cm⁻¹ and disappeared in the spectra of the complexes. The strong band at 1600 cm⁻¹ can be related to C=N and/or C=O bonds [18]. The IR spectra of the complexes show a strong band at 1470–1540 cm⁻¹ due to (C=N) [22,23]. The C=C vibrational frequencies appeared in the range of 1470–1500 cm⁻¹. These bands are shifted towards lower frequencies in the spectra of metal complexes compared with the free Schiff bases indicating the involvement of the azomethine nitrogen in chelation with the metal ions, the coordination of nitrogen to the metal ion would be expected to reduce the electron density of the azomethine link and thus causes a shift in the ν_(C=N) group [24]. The vibrational peak of coordinated water is in the range of 3400–3450 cm⁻¹.

Electronic absorption spectra

The electronic spectra of free ligands under study in ethanol solution were characterized mainly by three absorption bands in the region of 900–200 nm assigned to π–π* transition. In metal complexes, these transitions were found to be shifted to lower or higher energy region compared to the free ligands transitions confirming the coordination of the ligands to metal ions [17]. In addition, a d–d transition appeared in the range of 315–333 nm region.

¹H NMR spectra

The chemical shift (δ, ppm) of different protons of the Schiff base ligands is presented in Sections ‘Synthesis of 2-(3-hydroxy-1-methyl-but-2-enylideneamino)-phenol (H₂L¹), Synthesis of 2-(3-hydroxy-1-methyl-but-2-enylideneamino)-4-chlorophenol (H₂L²) and Synthesis of 2-(3-hydroxy-1-methyl-3-phenyl-prop-2-enylideneamino)-phenol (H₂L³)’.

The ¹H NMR of ligands is in line with the proposed structures. The NH/OH proton was seen in the range of 12.14–12.80 ppm as singlet. The phenolic hydrogen was seen in the range of 9.91–10.03 ppm as singlet. The proton of alkene was seen in the range of 5.18–6.02 ppm as singlet. The aromatic hydrogens were seen in 6.77–7.91 ppm region as multiplet. The hydrogens of methyl group were seen in 1.96–3.38 ppm region as singlet.

Thermogravimetric analyses

The thermal decomposition of the copper complexes showed characteristic pathways, depending on the nature of the ligands, as can be seen from the TG/DTA curves in Fig. 3. The absence of weight loss up to 80 °C indicates that there is no water molecule in the crystalline solid. In these complexes, the TG showed weight loss up to 250 °C indicates the presence of solvent molecule coordinated with complexes [25–27].

The complex of [CuL¹(H₂O)] decomposes in one step. The decomposition occurs up to about 250 °C and is attributed to the release of water and C₁₁H₁₁NO (TG = 69.30; calc. = 70.60%) resulted in the formation of the CuO at 349 °C (TG = 30.70%; calc. = 29.40%).

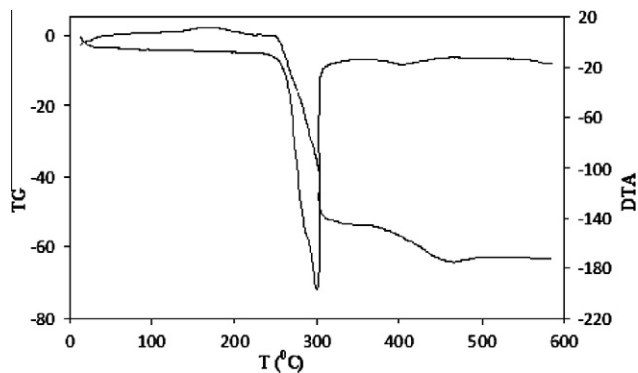


Fig. 3. TG and DTG curve of: $\text{CuL}^2(\text{H}_2\text{O})$.

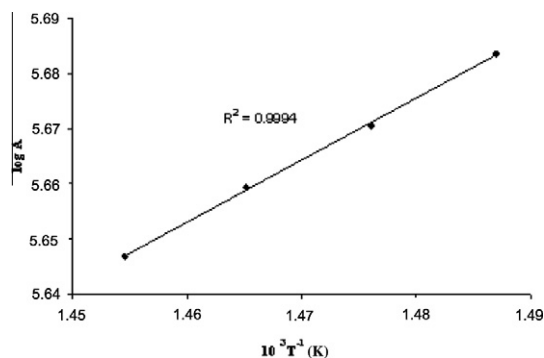


Fig. 4. Coats–Redfern plots of $[\text{CuL}^2(\text{OH}_2)]$ complex, step 1, $A = \frac{\log w_f}{T^2}$.

The complex of $[\text{CuL}^2(\text{H}_2\text{O})]$ decomposes in two steps. The first step occurs up to about 256 °C and is attributed to the release of water and $\text{C}_{10}\text{H}_{10}\text{N}$ (TG = 50.13; calc. = 51.20%). The second step of thermal decomposition which occurred in the range of 367–452 °C (TG = 9.50%; calc. = 11.10%), resulted in the formation of a mixture of CuO and CuCl_2 at 452 °C.

The complex of $[\text{CuL}^3(\text{H}_2\text{O})]$ decomposes in three steps. The first step occurred up to about 278 °C and was attributed to the release of water and $\text{C}_6\text{H}_4\text{NO}$ (TG = 35.70%; calc. = 37.30%). The second thermal event was observed between 335 and 370 °C (TG = 17.20%; calc. = 15.60%). The third mass loss between 375 and 444 °C was assigned to the rest of the ligand (TG = 21.70%; calc. = 23.10%) with the formation of the CuO (TG = 25.10%; calc. = 24.20%).

Kinetics aspects

All the well-defined stages were selected to study kinetics decomposition of the complexes. The kinetics parameters (the activation energy E and the pre-exponential factor A) were calculated using the Coats–Redfern equation [15],

$$\log \left[\frac{g(\alpha)}{T^2} \right] = \log \frac{AR}{\phi E} \left[1 - \frac{2RT}{E_a} \right] - \frac{E_a}{2.303RT} \quad (1)$$

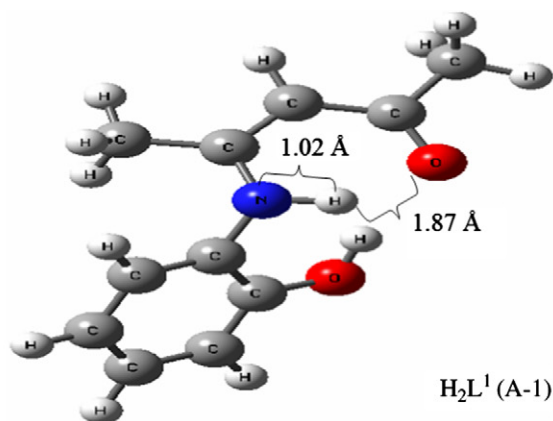
Table 1

Thermal and kinetics parameters for copper complexes.

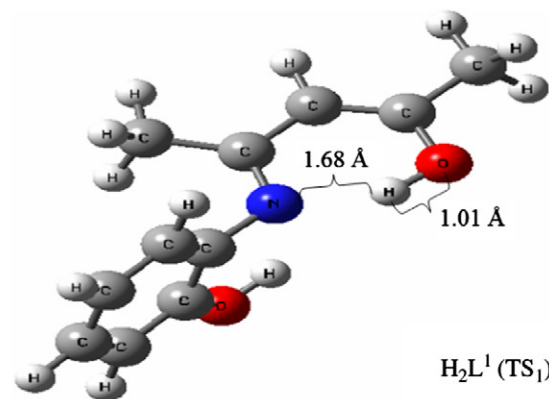
Compound	ΔT (°C) ^a	Percent (%) ^b	E^* (kJ/mol)	A^* (s ⁻¹)	S^* (kJ mol ⁻¹ K ⁻¹)	H^* (kJ/mol)	G^* (kJ/mol)
$\text{CuL}^1(\text{H}_2\text{O})$	250–349	69.30(70.60)	89.37	2.83×10^5	-141	86.87	129
$\text{CuL}^2(\text{H}_2\text{O})$	256–319	50.13(51.20)	117.73	2.00×10^8	-85	115.33	140
	367–452	9.50(11.10)	22.22	4.25×10^0	-236	18.81	115
$\text{CuL}^3(\text{H}_2\text{O})$	278–331	35.70(37.30)	201.79	9.66×10^{15}	61	199.29	181
	335–370	17.20(15.60)	81.02	1.23×10^6	-130	78.11	124
	375–444	21.70(23.10)	63.89	3.35×10^2	-199	60.51	142

^a The temperature range of decomposition pathways.

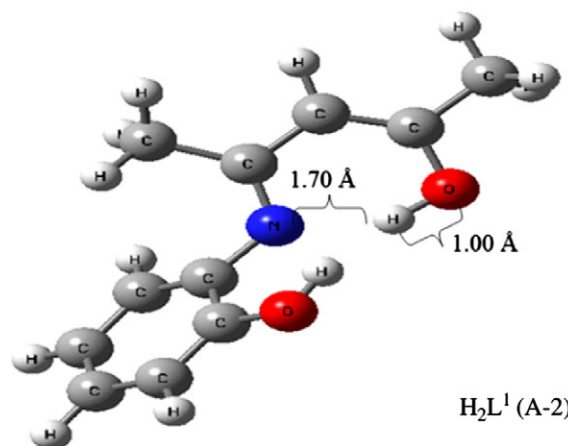
^b Percent of weight loss found (calculated).



H_2L^1 (A-1)



H_2L^1 (TS₁)



H_2L^1 (A-2)

Fig. 5. Optimized structures of H_2L^1 (A).

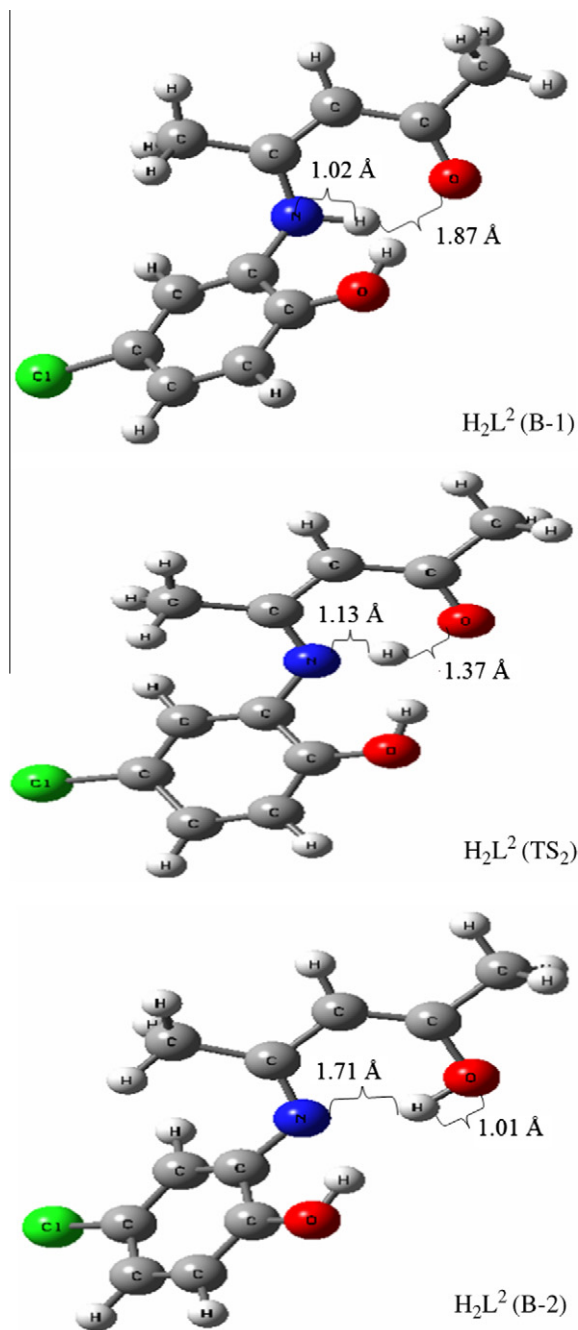


Fig. 6. Optimized structures of H₂L² (B).

where $g(\alpha) = [W_f]/(W_f - W)$. In the present case, a plot of L.H.S (left hand side) of this equation against $1/T$ gives straight line (Fig. 4) whose slope and intercept are used to calculate the kinetic parameters by the least square method. The goodness of fit was checked by calculating the correlation coefficient. The other systems and their steps show the same trend.

The entropy of activation S^\ddagger was calculated using the following equation

$$A = \frac{kT_s}{h} e^{\frac{S^\ddagger}{R}} \quad (2)$$

where k , h and T_s are the Boltzman's constant, the Planck's constant and the peak temperature, respectively. The enthalpy and free energy of activation were calculated using Eqs. (3) and (4).

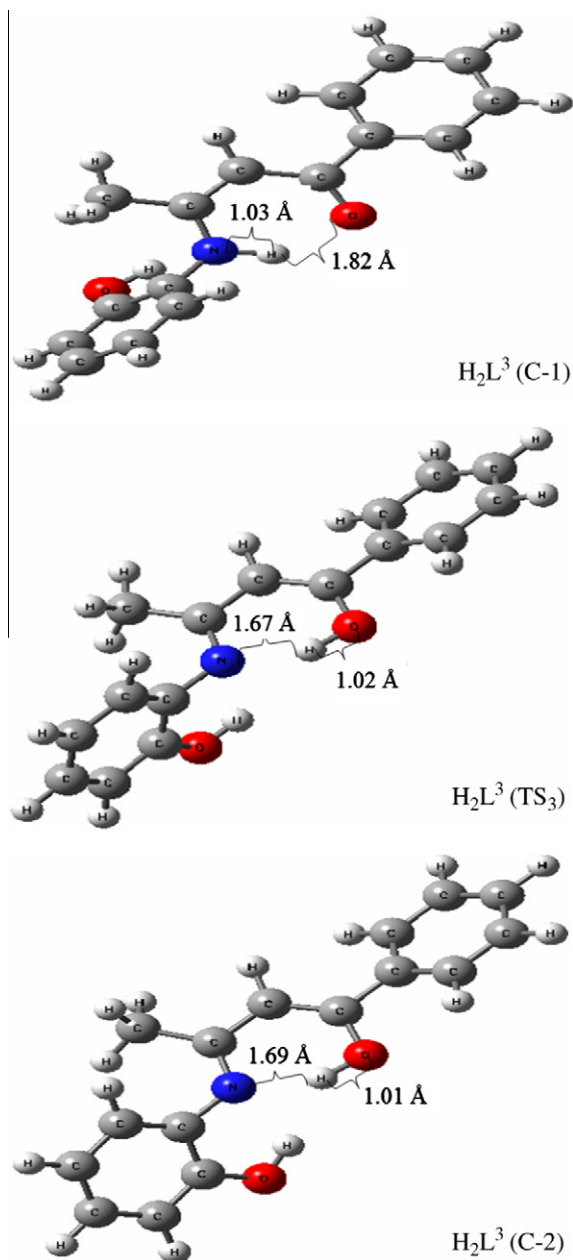


Fig. 7. Optimized structures of H₂L³ (C).

$$E_a = H^\ddagger + RT, \quad (3)$$

$$G^\ddagger = H^\ddagger - TS^\ddagger \quad (4)$$

The various kinetics parameters calculated are given in Table 1. The activation energy (E_a) in the different stages are in the range of 22.22–117.73 kJ mol⁻¹. The respective values of the pre-exponential factor (A) vary from 4.25×10^0 to 9.66×10^{15} s⁻¹. The corresponding values of the entropy of activation (S^\ddagger) are in the range of -236 to 61 J mol⁻¹. The corresponding values of the enthalpy of activation (H^\ddagger) are in the range of 18.81–199.39 kJ mol⁻¹. The corresponding values of the free energy of activation (G^\ddagger) are in the range of 115–181 kJ mol⁻¹. Due to the unstable intermediate the activation energy of the later stages for [CuL²(H₂O)] and [CuL³(H₂O)] were smaller than that of the first one. The negative values of entropy of activation indicate that the activated complex has a more ordered structure than the reactants [28,29].

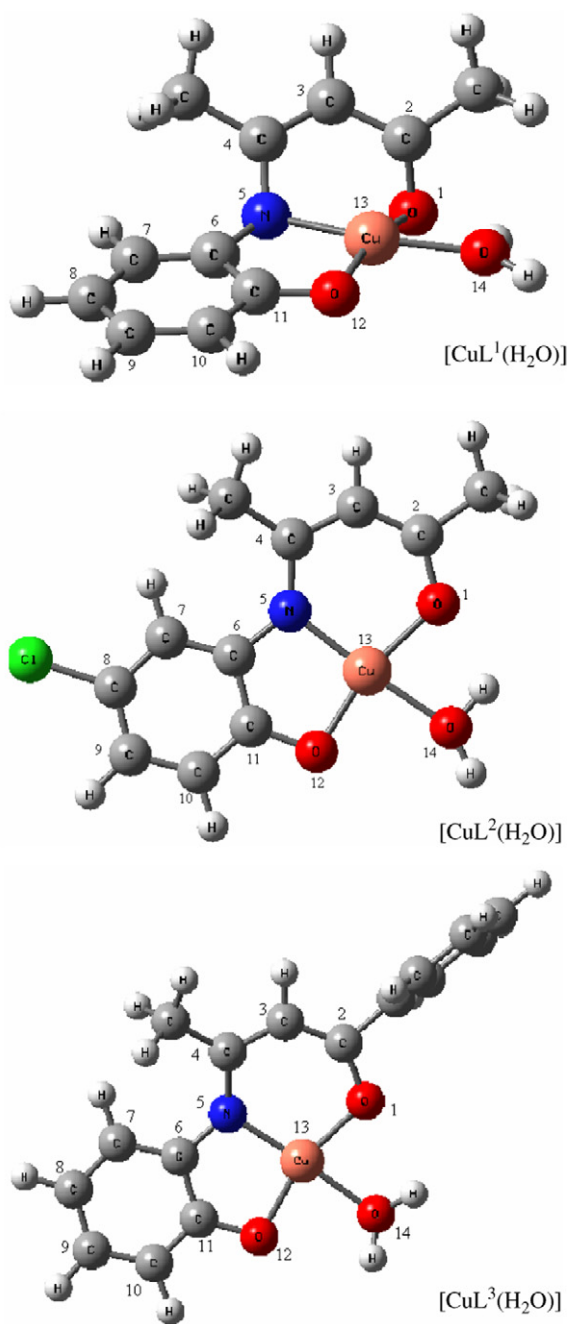


Fig. 8. Optimized structures of complexes.

Table 3

Significant bond lengths and bond angles calculated at the MP2 method with 6-31G(d) basis set for H, C, N and O atoms and LANL2DZ for the Cu atom.

Structural parameter	CuL ¹ (H ₂ O)	CuL ² (H ₂ O)	CuL ³ (H ₂ O)
<i>Bond lengths (Å)</i>			
O(1)–Cu(13)	1.86	1.88	1.87
N(5)–Cu(13)	1.90	1.88	1.89
O(12)–Cu(13)	1.88	1.84	1.88
O(14)–Cu(13)	1.93	1.95	1.97
O(1)–C(2)	1.42	1.36	1.36
C(11)–O(12)	1.34	1.36	1.36
<i>Bond angles (°)</i>			
O(1)–Cu(13)–N(5)	91.94	98.84	104.36
O(1)–Cu(13)–O(14)	77.39	77.50	79.01
N(5)–Cu(13)–O(12)	91.74	95.72	93.22
O(12)–Cu(13)–O(14)	98.95	87.94	83.41
O(1)–Cu(13)–O(12)	162.84	165.44	162.42
N(5)–Cu(13)–O(14)	169.20	176.25	176.38

Molecular structure and analysis of bonding modes

The structures of the ligands were determined by ab initio calculations. The different tautomerism conversion was investigated to compare the stability of the different tautomers and the best structure conformers for the ligands and the geometry of copper complexes.

The geometries of the Schiff base ligands and complexes are represented in Figs. 5–8. Significant bond lengths and bond angles are also reported in Tables 2 and 3. It is shown that in the complexes, Cu(II) ion is in square-planar NO₃ coordination geometry. Because of the different character of the atoms forming around the Cu(II) ion, the coordination square is distorted. The bond angle of O(1)–Cu(13)–O(14) is smaller than O(1)–Cu(13)–N(5), N(5)–Cu(13)–O(12) and O(12)–Cu(13)–O(14). It may be due to the intramolecular hydrogen bonds between the enolate oxygen with the hydrogens of the H₂O molecule in the proposed structure.

In this article, we also investigated the reactions R1, R2 and R3 which are hydrogen abstraction reaction by oxygen or nitrogen atoms. Schematic potential energy diagram at the B3LYP/6-31G(d) level is shown in Fig. 9. The calculated relative energies at theory level mentioned above are shown in Fig. 10. In the reaction R1 oxygen number 1 in the A-1 structure receives hydrogen from N–H bond to produce A-2. This reaction proceeds through transition states TS₁ with imaginary frequency 1150.5i cm⁻¹. As demonstrated in Figs. 9 and 10, the barrier energy for this reaction is 15.4 kJ mol⁻¹. It was shown that the structure of A-1 is 12.9 kJ mol⁻¹ more stable than the structure of A-2 for H₂L¹ ligand. There are similar pathways in R2 and R3 reactions, with transition state in the top of minimum energy path, TS₂ and TS₃ for which the imaginary frequencies are 1125.8i cm⁻¹ and 1249.4i cm⁻¹ and the

Table 2

Significant bond lengths and bond angles calculated at the MP2/6-31G(d) level.

Structural parameter	H ₂ L ¹				H ₂ L ²			H ₂ L ³		
	A-1	TS ₁	A-2	X-ray ^a	B-1	TS ₂	B-2	C-1	TS ₃	C-2
<i>Bond lengths (Å)</i>										
O(1)–C(2)	1.26	1.34	1.34	1.27	1.26	1.27	1.34	1.26	1.34	1.34
C(4)–N(5)	1.37	1.31	1.31	1.34	1.37	1.34	1.31	1.37	1.32	1.31
N(5)–C(6)	1.42	1.42	1.41	1.41	1.42	1.41	1.41	1.43	1.42	1.41
C(11)–O(12)	1.36	1.37	1.37	1.37	1.36	1.36	1.36	1.37	1.37	1.37
<i>Bond angles (°)</i>										
C(4)–N(5)–C(6)	123.77	118.65	122.22	131.50	123.78	128.77	122.22	122.73	118.70	122.53
N(5)–C(6)–C(7)	122.23	122.07	124.32	124.72	121.73	122.52	123.92	122.14	122.06	124.45
C(6)–C(11)–O(12)	123.01	120.75	120.58	115.94	123.30	121.84	120.68	120.89	120.79	120.65
C(10)–C(11)–O(12)	117.71	118.98	119.09	123.60	117.68	117.11	119.16	119.06	118.97	119.00

^a X-ray data for H₂L¹ taken from Ref. [10].

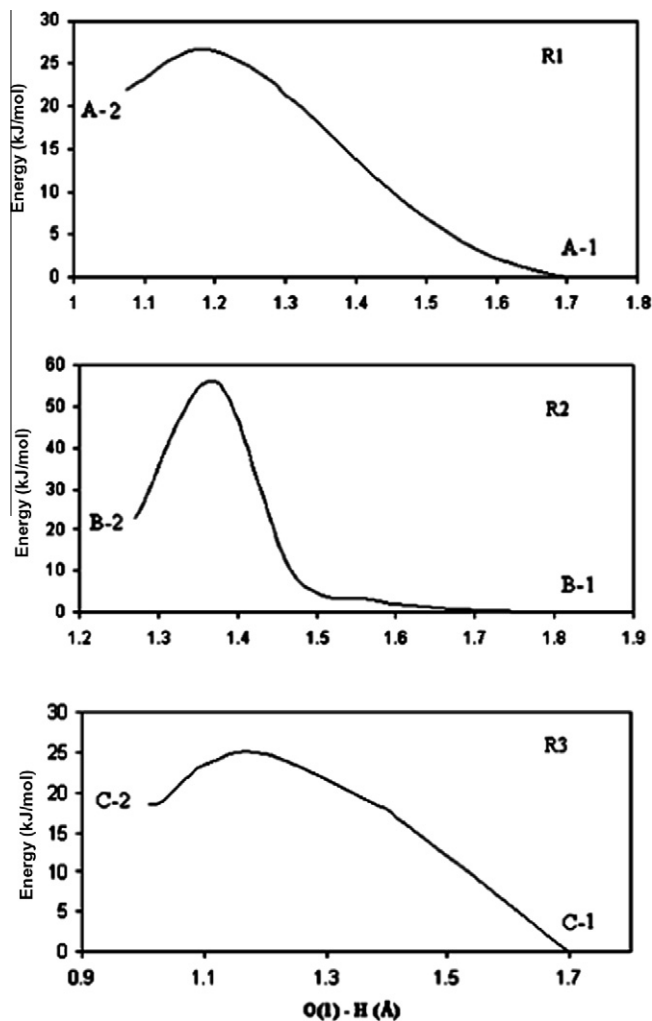


Fig. 9. Potential energy surface for R1, R2 and R3 reactions.

barrier energies are 20.1 kJ mol^{-1} and 21.5 kJ mol^{-1} , respectively. Relative energies of different species which were corrected with zero point energies are shown in these structures. The results show that keto-amine (B-1 and C-1) structures are more stable than enol-imine (B-2 and C-2) for H_2L^2 and H_2L^3 ligands, respectively.

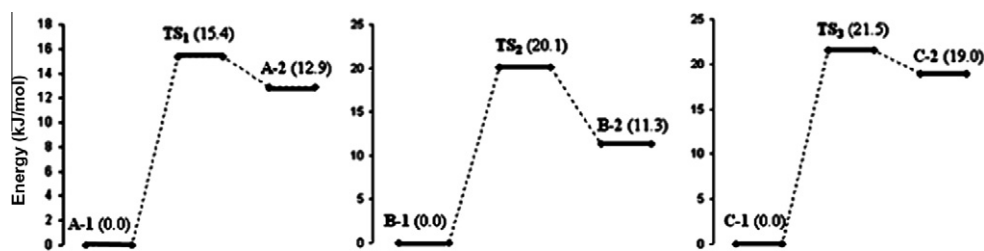


Fig. 10. Relative energies of different species for reactions R1, R2 and R3 in kJ mol^{-1} at the MP2/6-31G(d) level. All values are corrected with zero point energies.

Table 4
Relative energies (with zero point energy correction) ΔE (kJ mol^{-1}), zero point energies ZPE (kJ mol^{-1}) and dipole moments μ (D) of the isomers of ligands calculated at the MP2 level using a 6-31G(d) basis set.

H_2L^1	ΔE	ZPE	μ	H_2L^2	ΔE	ZPE	μ	H_2L^3	ΔE	ZPE	μ
A-1	0.0	584.5	3.36	B-1	0.0	559.4	3.27	C-1	0.0	726.5	2.29
TS ₁	15.4	582.5	3.03	TS ₂	20.1	559.3	2.79	TS ₃	21.5	722.7	3.26
A-2	12.9	583.6	3.45	B-2	11.3	558.1	3.89	C-2	19.0	724.1	3.58

Table 5

Energy of activation for forward reaction $E_{a,f}$ (kJ mol^{-1}), energy of activation for reverse reaction $E_{a,r}$ (kJ mol^{-1}), standard free energy for forward reaction ΔG_f^0 (kJ mol^{-1}), standard free energy for reverse reaction ΔG_r^0 (kJ mol^{-1}), equilibrium constant for forward reaction K_f and equilibrium constant for reverse reaction K_r for R1, R2 and R3 reactions.

Energy	Rn		
	R1	R2	R3
$E_{a,f}$	15.4	20.1	21.5
$E_{a,r}$	2.5	8.8	2.6
ΔG_f^0	14.0	11.1	19.5
ΔG_r^0	-14.0	-11.1	-19.5
K_f	3.50×10^{-3}	0.01	3.85×10^{-4}
K_r	285.75	89.59	259.12

The relative energies were corrected with zero point energies. Zero point energies and dipole moments of the individual isomers of ligands are presented in Table 4.

Standard free energies, activation energies and equilibrium constants for the forward and reverse of R1, R2 and R3 reactions were reported in Table 5.

The Arrhenius equation is

$$k = A \exp(-E_a/RT) \quad (5)$$

where k is the rate constant, E_a is the activation energy, A is pre-exponential factor, R is the gas constant and T is temperature. According to this equation and the above results (Table 5), $k(R1)$ in the forward and reverse directions are greater than $k(R2)$ and $k(R3)$.

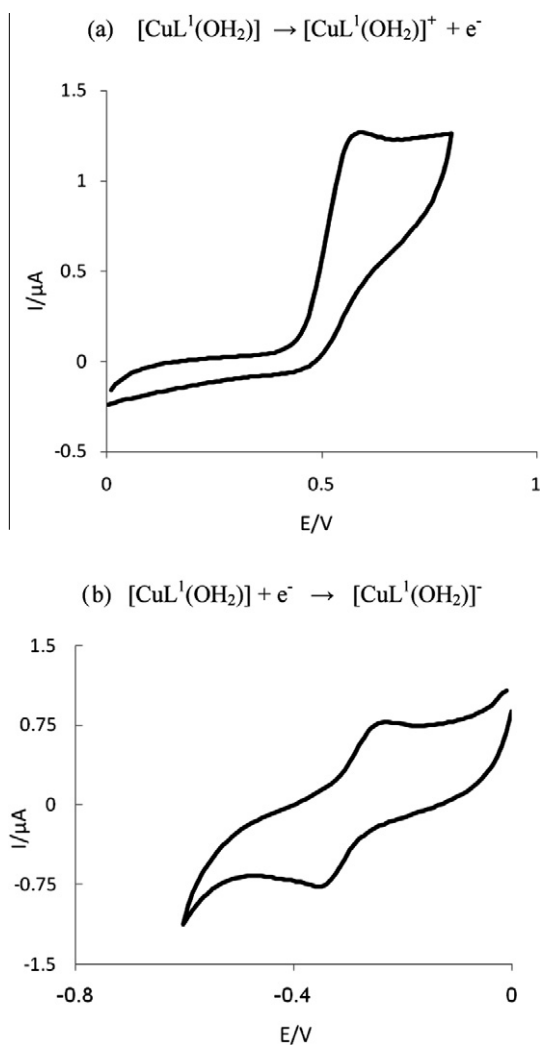
Equilibrium constant for these reactions are also calculated to show the ratio of concentration of products to concentration of reactants.

Natural bond orbital (NBO) analysis yields valuable information concerning the electronic structure of ligands and their metal complexes. In ligand H_2L^1 , N(5)–H, O(1)–H and the phenolic O(12)–H are polar covalent bonds with -0.70 , -0.79 and -0.76 charges, respectively. In the complex $\text{CuL}^1(\text{H}_2\text{O})$, Cu(13)–N(5), Cu(13)–O(1) and Cu(13)–O(12) bonds are ionic with -0.52 , -0.98 and -0.98 charges on the coordinated nitrogen and oxygens, respectively. The negative charge on nitrogen coordinated to metal was less than the free ligand. The other systems show the same trends. The atomic charges are represented in Table 6 which are from natural population analysis (NPA) for ligands and the metal complexes with NO_3 coordination. It could be argued that the amine form of

Table 6

Atomic charges (e) calculated from natural population analysis at the MP2/6-31G(d) level.

Atom	Compound								
	A-1	A-2	D	B-1	B-2	E	C-1	C-2	F
N(5)	-0.70	-0.70	-0.52	-0.71	-0.70	-0.69	-0.74	-0.69	-0.62
O(1)	-0.78	-0.79	-0.98	-0.77	-0.78	-1.01	-0.74	-0.78	-1.02
O(12)	-0.76	-0.76	-0.98	-0.76	-0.76	-0.99	-0.76	-0.76	-0.96
O(14)	-	-	-1.08	-	-	-1.06	-	-	-1.02
Cu(13)	-	-	1.67	-	-	1.66	-	-	1.66

**Fig. 11.** Cyclic voltammogram of $[\text{CuL}^1(\text{OH}_2)]$, in acetonitrile at room temperature. Scan rate: 100 mV/s.

ligands is dominant while the imine form is more dominant in the complexes.

Electrochemistry

The electrochemical properties of copper complexes were investigated in acetonitrile. The CV diagrams for the $[\text{CuL}^1(\text{H}_2\text{O})]$ were shown in Fig. 11 and the potentials were listed on Table 7. For all complexes one anodic peak is observed in potential range from +0.58 to +0.80, but no evidence for a corresponding cathodic peak is observed, except for the $[\text{CuL}^3(\text{H}_2\text{O})]$ complex. In the negative potential scan, a cathodic peak is observed for the studied complexes in the potential range from -0.34 to -1.04 V. In this

Table 7

Redox potential data of Cu(II) complexes in acetonitrile solution.

Compound	E_{pa} (II → III)	E_{pc} (III → II)	E_{pc} (II → I)	E_{pa} (I → II)
$\text{CuL}^1(\text{H}_2\text{O})$	0.58	-	-0.34	-0.25
$\text{CuL}^2(\text{H}_2\text{O})$	0.63	-	-0.40	-0.17
$\text{CuL}^3(\text{H}_2\text{O})$	0.82	0.64	-1.04	-

case, the corresponding anodic peak is observed in the range from -0.17 to -0.25 V, except for $[\text{CuL}^1(\text{H}_2\text{O})]$ complex, which shows totally irreversible behaviour.

The anodic and cathodic process contain one peak in oxidation and reduction area and show that, the synthesized complexes contains one copper atom in a monomer form [30,31].

Conclusions

Considering the spectroscopy, thermogravimmetrical and ab initio calculations over the Schiff base ligands and copper complexes showed the following results.

1. The IR, ^1H NMR and elemental analysis confirmed that the synthesised ligands and complexes contain the proposed formula.
2. The thermal decomposition pathways of the studied Schiff base complexes are first order in all steps.
3. The keto-amine is more stable than the enol-imine form of the ligands.
4. Keto-amine and enol-amine forms can convert to each other via a transition state.
5. In the complexes, Cu(II) ion has square-planar NO_3 coordination geometry.

References

- [1] L. Canali, D.C. Sherrington, Chem. Soc. Rev. 28 (1998) 85–95.
- [2] A.A. Isse, A. Gennaro, E. Vianello, J. Electroanal. Chem. 444 (1998) 241–245.
- [3] D. Pletcher, H. Thompson, J. Electroanal. Chem. 464 (1999) 168–175.
- [4] T. Okada, K. Katou, T. Hirose, M. Yuasa, I. Sekine, J. Electrochem. Soc. 146 (1999) 2562–2568.
- [5] M.H. Habibi, E. Shojaee, G.S. Nichol, Spectrochim. Acta A 98 (2012) 396–404.
- [6] S.J. Lippard, J.M. Berg, Principles of Bioinorganic Chemistry, University Science Books, California, 1994, and references cited therein.
- [7] D.E. Fenton, Bioinorganic Chemistry, Oxford University Press, Oxford, 1995, and references cited therein.
- [8] Y. Yoshikawa, E. Ueda, K. Kawabe, K. Miyabe, T. Takino, H. Sakurai, Y. Kojima, J. Biol. Inorg. Chem. 7 (2002) 68–73.
- [9] M.H. Habibi, E. Askari, M. Amirnasr, A. Amiri, Y. Yamane, T. Suzuki, Spectrochim. Acta A 79 (2011) 666–671.
- [10] J.P. Glusker, A.K. Katz, C.W. Bock, Rigaku J. 16 (1999) 8–16.
- [11] A.H. Kianfar, S. Zargari, J. Coord. Chem. 61 (2008) 341–352.
- [12] S. Basu, G. Gupta, B. Das, K.M. Rao, J. Organometallic Chem. 695 (2010) 2098–2104.
- [13] K.V. Hecke, V.T. Ngan, P. Nockemann, B. Thijs, M.T. Nguyen, K. Binnemans, L.V. Meervelt, J. Mol. Struct. 885 (2008) 97–103.
- [14] A.M. Amado, P.J.A. Ribeiro-Claro, J. Inorg. Biochem. 98 (2004) 561–568.
- [15] A.W. Coats, J.P. Redfern, Nature 201 (1964) 68–69.
- [16] M.J. Frisch, G.W. Trucks, H.B. Schlegel, G.E. Scuseria, M.A. Robb, J.R. Cheeseman, J.A. Montgomery, Jr., T. Vreven, K.N. Kudin, J.C. Burant, J.M. Millam, S.S. Iyengar,

- J. Tomasi, V. Barone, B. Mennucci, M. Cossi, G. Scalmani, N. Rega, G.A. Petersson, H. Nakatsuji, M. Hada, M. Ehara, K. Toyota, R. Fukuda, J. Hasegawa, M. Ishida, T. Nakajima, Y. Honda, O. Kitao, H. Nakai, M. Klene, X. Li, J.E. Knox, H.P. Hratchian, J.B. Cross, C. Adamo, J. Jaramillo, R. Gomperts, R.E. Stratmann, O. Yazyev, A.J. Austin, R. Cammi, C. Pomelli, J.W. Ochterski, P.Y. Ayala, K. Morokuma, G.A. Voth, P. Salvador, J.J. Dannenberg, V.G. Zakrzewski, S. Dapprich, A.D. Daniels, M.C. Strain, O. Farkas, D.K. Malick, A.D. Rabuck, K. Raghavachari, J.B. Foresman, J.V. Ortiz, Q. Cui, A.G. Baboul, S. Clifford, J. Cioslowski, B.B. Stefanov, G. Liu, A. Liashenko, P. Piskorz, I. Komaromi, R.L. Martin, D.J. Fox, T. Keith, M.A. Al-Laham, C.Y. Peng, A. Nanayakkara, M. Challacombe, P.M.W. Gill, B. Johnson, W. Chen, M.W. Wong, C. Gonzalez, J.A. Pople, Gaussian 03, Revision A.1, Gaussian, Inc., Pittsburgh PA, 2003.
- [17] Z.H. Abd El-Wahab, *Spectrochim. Acta A* 67 (2007) 25–38.
- [18] Ch. Yu-Ying, E.Ch. Doris, B.D. McKinney, L.J. Willis, S.C. Cumming, *Inorg. Chem.* 20 (1981) 1885–1892.
- [19] E. Kwiatkowski, M. Kwiatkowski, *Inorg. Chim. Acta* 82 (1984) 101–109.
- [20] J.P. Costes, M.I. Fernandez-Garcia, *Inorg. Chim. Acta* 237 (1995) 57–63.
- [21] A.D. Garnovskii, A.L. Nivorozhkin, V.I. Minkin, *Coord. Chem. Rev.* 126 (1993) 1–69.
- [22] A. Bottcher, T. Takeuchi, I. Hardcastle, T.J. Mead, H.B. Gray, D. Cwikel, M. Kapon, Z. Dori, *Inorg. Chem.* 36 (1997) 2498–2504.
- [23] M. Asadi, A.H. Sarvestani, Z. Asadi, M. Setoodekhah, *Syn. React. Inorg. Metal-Org. Nano-Metal Chem.* 35 (2005) 639–644.
- [24] Z.H. Abd El-Wahab, M.M. Mashaly, A.A. Salman, B.A. El-Shetary, A.A. Faheim, *Spectrochim. Acta A* 60 (2004) 2861–2873.
- [25] A.H. Kianfar, L. Keramat, M. Dostani, M. Shamsipur, M. Roushani, F. Nikpour, *Spectrochim. Acta A* 77 (2010) 424–429.
- [26] B.S. Garg, D.N. Kumar, *Spectrochim. Acta A* 59 (2003) 229–234.
- [27] A. Anthonysamy, S. Balasubramanian, *Inorg. Chem. Commun.* 8 (2005) 908–911.
- [28] S. Mathew, C.G.R. Nair, K.N. Ninan, *Thermochim. Acta* 155 (1989) 247–253.
- [29] M.K.M. Nair, P.K. Radhakrishnan, *Thermochim. Acta* 261 (1995) 141–149.
- [30] S. Meghdadi, K. Mereiter, V. Langer, A. Amiri, R.S. Erami, A.A. Massoud, M. Amirnasr, *Inorg. Chim. Acta* 385 (2012) 31–38.
- [31] E. Pereira, L.R. Gomes, J.N. Low, B. de Castro, *Polyhedron* 27 (2008) 335–343.